Biomimetic triblock copolymer membranes: from aqueous solutions to solid supports†

Alfredo González-Pérez,*[a] Valeria Castelletto,[b] Ian W. Hamley[b] and Pablo Taboada[c]

Received 22nd July 2010, Accepted 10th November 2010
DOI: 10.1039/c0sm00711k

In the present paper, we studied the preparation of biomimetic triblock copolymer (ABA) membranes in aqueous solution and their deposition into solid supports. The self-assembly structures of the ABA in aqueous solution was investigated by using optical microscopy, dynamic light scattering, electron microscopy (EM) and SAXS. Spherical and tubular polymersomes were found at the highest concentrations investigated. The mechanism of deposition on solid supports (mica and glass) was elucidated by using atomic force microscopy (AFM). The deposition results in the formation of a uniform defect-free membrane at suitable polymer concentrations.

Introduction

Structures from nature have remarkable properties, many of which have inspired laboratory research. (Bio)inspired materials and devices are attracting increasing interest because of their unique properties, which have paved the way to many significant applications.[1–3] One of the bottom-up strategies for creating such structured materials is to utilize spontaneous self-assembly of macromolecules. One promising class of these building molecules is block copolymers, which are macromolecules formed by covalently linking two or more chemically distinct polymeric blocks. Block copolymers have been the subject of extensive research during recent years as a result of their very rich physico-chemical behavior, the vast range of nanostructures they can generate either in solid or liquid state, and the fine control which can be exerted by simply tuning copolymer architecture, composition, block lengths, temperature…[4,5]

Amongst different bioinspired nanostructures and (bio)-applications block copolymers have been tested for, special attention has been paid to mimic biological membranes.[6] Most of the studies in membrane protein reconstitution have been done using supported or tethered membranes based on lipids because they are able to efficiently mimic the cell membranes present.[7] The advantages of using polymers are the outstanding stability of the resulting membrane, which can be additionally improved both by changing the chemical structure of the macromolecule and cross-linking the polymer after membrane formation. In addition, it is also possible to tune the membrane thickness by using polymers to obtain values about two or three times larger than artificial membranes based on lipids. In this regard, it was recently demonstrated that triblock copolymer membranes based on poly(dimethylsiloxane) (PDMS) and poly(2-methyloxazoline) (PMOXA) blocks can be used to incorporate membrane proteins that maintain their activity after insertion as also occurred in biological lipid-based membranes.[8,9] These polymeric membranes accommodate the membrane protein by reducing the hydrophobic thickness to values close to that of lipid membranes, while the rest of the membrane retains the original thickness. This fact can avoid the direct contact between the membrane protein and the substrate by creating an effective reservoir of solvent between the protein and the substrate.

One of the drawbacks of the solid supported membranes is that the proximity to the solid support is not usually enough to avoid the direct contact between the membrane proteins and the support, which can result in protein denaturation. This problem can be avoided by separating the artificial membrane from the support using soft polymeric materials. Recently, González-Pérez *et al.*[10] showed that ABA triblock copolymers of poly-(dimethylsiloxane) (PDMS) and poly(2-methyloxazoline) PMOXA blocks can be used to prepare free-standing block copolymer membranes that allow the incorporation of functional gramicidin A. In this work, the solution was prepared in decane because of the low solubility of the ABA block copolymer in aqueous solution. In order to avoid undesired solvent effects in the membrane protein structure a more appropriate solvent should be used.

In the present work we investigate the mechanism of membrane formation by a triblock copolymer of PDMS and PMOXA, $PMOXA_7$-$PDMS_{60}$-$PMOXA_7$ (type ABA, where the subscripts denote the block lengths), as well as the structural aspects that maintain the outstanding stability of the formed polymeric membrane in a large area. Since the solubility of the present ABA block copolymer in water is concentration-dependent; at low concentration the polymer solution was found to present a homogenous milky appearance and colloidal stability. This opens additional possibilities to use organic solvent-free membranes as a support for membrane protein incorporation, which might avoid alterations in the membrane protein structure as a consequence of the presence of organic solvents. Thus, prior to membrane formation studies it was necessary to analyze in detail the self-assembled structures formed in aqueous solution

[a]*Membrane Biophysics Group, Niels Bohr Institute, University of Copenhagen, Blegdamsvej 17, 2100 Copenhagen Ø, Denmark. E-mail: gonzalez@nbi.ku.dk; alfredogp@gmail.com*
[b]*School of Chemistry, Food Science and Pharmacy, University of Reading, Whiteknights, Reading, RG6 6AD, UK*
[c]*Department of Condensed Matter Physics, Faculty of Physics, University of Santiago de Compostela, 15782 Campus Sur, Santiago de Compostela, Spain*

† Electronic supplementary information (ESI) available: Figures X1–X3. See DOI: 10.1039/c0sm00711k

by the present block copolymer. Dynamic light scattering (DLS), small-angle X-ray scattering (SAXS) and optical, confocal and transmission electron microscopies (TEM) have been used to characterize the polymersomes in aqueous solution. We found a coexistence of both spherical and tubular vesicles, the relative population of which depends on the polymer concentration. The formation of block copolymer membranes prepared from aqueous solutions onto two solid supports (mica and glass) and their structural characteristics were determined by atomic force microscopy (AFM) experiments have been performed to characterize the ABA membranes on mica and glass. The interaction between polymeric membranes and solid substrates become a key step in the development of new solid supported membranes containing membrane proteins embedded. Previously, we showed a large surface area in an array of 64 apertures can be used in electrophysiological studies and represents an alternative to conventional lipid based black lipid membranes (BLMs) that have lower mechanical stability.[10] The promising perspectives and new applications in protein screening and protein function studies depend on the standardization of systems such as the present one for different ion channels and other membrane proteins.

Experimental

Materials and methods

A triblock copolymer consisting of a middle block of 60 units of poly(dimethylsiloxane) (PDMS) and two 7 unit side blocks of poly(2-methyloxazoline) (PMOXA) carrying methacrylate end groups with a total molecular weight (MW) of 5800 g/mol ($PMOXA_7$-$PDMS_{60}$-$PMOXA_7$) (in short ABA) was obtained from BioCure (USA), and used as received. For polymer solution preparation, we dissolved an appropriate amount of the ABA copolymer in bidistilled water. All the samples were kept at room temperature. After the mixing was completed a milky solution was observed for all samples. Two microliters of each sample was used to prepare the membranes in the solid supports.

Optical microscopy

The optical images have been made using a Primo Star ALL from Zeiss. Complete configuration with full-Köhler stand including halogen illumination with a 6 V 30 W halogen lamp, a 4-position nosepiece tilted backwards, a mechanical stage 75 × 30 mm, and a specimen holder with spring clip left. Images were obtained with 4×, 10×, 40× and 100× Plan-Achromat objetives.

Laser scanning confocal microscopy (LCSM)

Experiments were performed on a Leica TCS SP2 confocal system mounted on a Leica DM-IRE2 upright microscope, using an objective ×63 for a glycerol-immersion lens. For LSCM, 2.4 mg/ml solutions were dyed using Rhodamine B (RhoB), such that each sample examined had a 2.6×10^{-4} wt % RhoB content. The excitation wavelength generated by an Argon laser was 514 nm, while the emission detection was in the range 558–617 nm. Samples put between a glass slide and a coverslip.

Dynamic light scattering

DLS experiments have been performed using a Brookhaven instrument with a thermostatic bath that allows temperature control. The stock solution was prepared at room temperature and filtrated using a filter pore of 800 nm. The equilibration time was 2 min between experiments. DLS correlation data were analyzed by the constrained regularized CONTIN method to obtain distributions of decay rate.[11] The hydrodynamic radius R_h was estimated from the diffusion coefficient using the Stokes–Einstein equation and assuming that the solvent viscosity is that of water:

$$D_0 = k_B T / 6\pi\eta R_h \quad (1)$$

where D_0 is the diffusion coefficient of a sphere at infinite dilution, k_B the Boltzmann constant, T the absolute temperature, and η the solvent viscosity.

Transmission electron microscopy

Suspensions (a drop) of aqueous micellized copolymer solutions at different copolymer concentrations were applied to an electron microscope copper grid, blotted, washed, negatively stained with 2% (w/v) of phosphotungstic acid, washed and evaporated under air. After drying, electron micrographs of the sample were obtained with a Phillips CM-12 electron microscope operating at 120 kV.

Small angle X-ray scattering (SAXS)

SAXS experiments were performed on beamline ID02 at the European Synchrotron Radiation Facility, Grenoble, France. Samples were mounted in a flow-through capillary cell, consisting of a 2 mm thick quartz capillary. A CCD detector was used to collect two-dimensional images which were reduced by radial integration to one-dimensional profiles. The sample–detector distance was 1.5 m. Subtraction of background scattering using a water reference was performed to obtain the corrected intensity, I(q), presented here.

Atomic force microscopy on glass substrates

The AFM set up used for the experiments with glass supports was composed of a PicoSPM head, a piezoelectric AFM scanner (30μm), and a cantilever for soft tapping mode PPP-NCST Nanosensors PointProbe®. The images were analyzed using PicoScan 5.3.3 software from Agilent Technologies (Santa Clara, California).

Atomic force microscopy on mica substrates

Tapping Mode AFM in air was performed on a Multimode™ SPM (Nanoscope IIIa, Digital Instruments). Samples were deposited on freshly cleaved mica. For imaging a solution, a drop of solution was left to incubate for two minutes and dried by capillarity immediately after. Experiments were run at ambient temperature using a J tube scanner (scan size: 10 × 10 μm, vertical range: 5 μm). Microfabricated crystal silicon probes with a spring constant of 20–80 N/m and a resonant frequency of 281–319 kHz (Veeco MPP-11100) were used as received. Z-scale

accuracy was checked once a day by means of a silicon grating (TGZ02 silicon grating, from Ultrasharp Cantilevers and Gratings) ensuring a nominal height deviation less than 2% at the highest scan size. The calibration of the scanner was confirmed by using a standard grid with well known dimensions (see Supporting Information Figure X1). To eliminate imaging artefacts, the scan direction was varied to ensure a true image. Images were obtained from at least five macroscopically separated areas on each sample. All images were processed using procedures for plane-fitting and flattening in the WSxM 4.0 Develop 11.4 software[12] without any filtering. All experiments were carried out at room temperature.

Theory

SAXS

The coherent part of the SAXS intensity from an isotropic solution of globular objects, $I(q)$, can be written as:[13]

$$I(q) = kP(q)S(q) \tag{2}$$

where k is a normalization constant proportional to the number density of scatterers, $P(q)$ is the form factor, $S(q)$ is the structure factor and q is the scattering vector given by $q = 4\pi\ sin\theta/\lambda$. The systems studied in this work correspond to widely separated systems. Therefore $S(q) \sim 1$ in eqn (1), so $I(q)$ is proportional to the form factor $P(q)$. For dilute systems, the scattering at low q obeys the Guinier law[14]

$$\lim_{q\to 0} I(q) = I(0)\exp\left(-\frac{q^2 R_{g,G}^2}{3}\right) \tag{3}$$

where $I(0)$ is the scattering at $q = 0$. The radius of gyration of the scattering particle, $R_{g,G}$, in eqn (2) can be evaluated from a $ln[I(q)]$ *vs* q^2 Guinier plot in the regime $qR_{g,G} < 1$.

The information extracted from eqn (2) can be complemented by calculating the distance distribution function $p(r)$ given by:[15]

$$p(r) = \frac{r^2}{2\pi}\int_0^\infty \frac{I(q)q^2\sin(qr)}{qr}\,dq \tag{4}$$

which provides information about the shape of the particle and goes from zero for distances higher than the maximum diameter of the particle D_{max}. The $p(r)$ function also provides the value of the radius of gyration $R_{g,I}$ of the particle through the integral relation:[15]

$$R_{g,I}^2 = \frac{\int_0^\infty p(r)r^2 dr}{2\int_0^\infty p(r)dr} \tag{5}$$

Results and discussion

ABA in aqueous solutions

It was recently reported by Grumelard *et al.* [9,16] that the ratio between the PMOXA and PDMS blocks determine the morphology the polymer can form in aqueous solution. According to this, our triblock polymer ABA should be able to form tubular vesicles in aqueous solution. At this point, we face two challenges: the investigation of the self-assembled structure formed by the ABA copolymer in both aqueous bulk solution and upon its deposition as a layer or membrane on a solid support from the bulk solution. Both steps are necessary to understand the unexpected nature of block copolymer membrane stability as well as the mechanism of fusion in solid supports resulting in single membranes.

In order to elucidate how the block copolymer self-assembled structure is affected by concentration we prepare a series of block copolymer samples at different concentrations. As a first approximation, we investigate some of the samples at room temperature, mainly those with a milky aspect using an optical microscope. An optical image from a solution of 20 mg/mL is shown in Fig. 1.

The image shows the presence of giant tubular polymersomes. This result is in good agreement with the rule reported by Grumelard *et al.*,[9,16] as previously commented. Using DLS measurements we determine the aggregate size distribution of a set of samples with concentrations ranging from 2.8 mg/mL to 20 mg/mL in aqueous solution. The particle sizes of the different samples were measured without previous filtration after being stored for 20 days at room temperature. In this regard, it is worth mentioning that from CONTIN analysis of DLS data we found a main population distribution with mean sizes ranging between 100–200 nm and other populations with larger sizes are also present, but their number-weight is rather low. For this reason, in Fig. 2 we only considered the behavior observed for the most populated species.

In Fig. 2a we can observe that below 7.5 mg/mL the sample contains a well defined particle size corresponding to approximately 100 nm. Nevertheless, above this concentration the samples show higher polydispersity as a consequence of the existence of different size populations, ranging from 100 to 200 nm. At the highest concentrations investigated (18–20 mg/mL) sizes unexpectedly drop to lower values of *ca.* 150 nm. Further analysis using the Cumulant method also showed a high degree of polydispersity that can be an additional indication of a second population with higher values out of the scale shown in the figure.

On the other hand, the size evolution of aggregates (polymersomes) of the PMOXA-PDMS-PMOXA block copolymer with time is also concentration-dependent. In this regard, for concentrations below 7.5 mg/mL the aggregate sizes increase

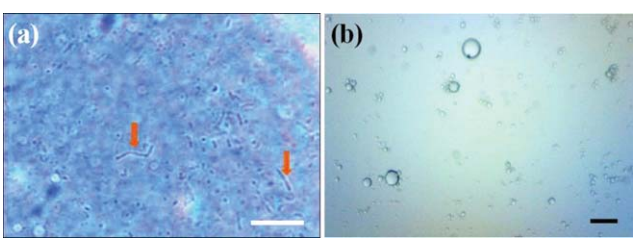

Fig. 1 Optical microscopy images of an aqueous solution of ABA (20 mg/mL) at room temperature at two different magnifications. (a) The orange arrows showing giant tubular polymersomes. (b) Shows giant spherical polymersomes. (Scale bar 25 μm).

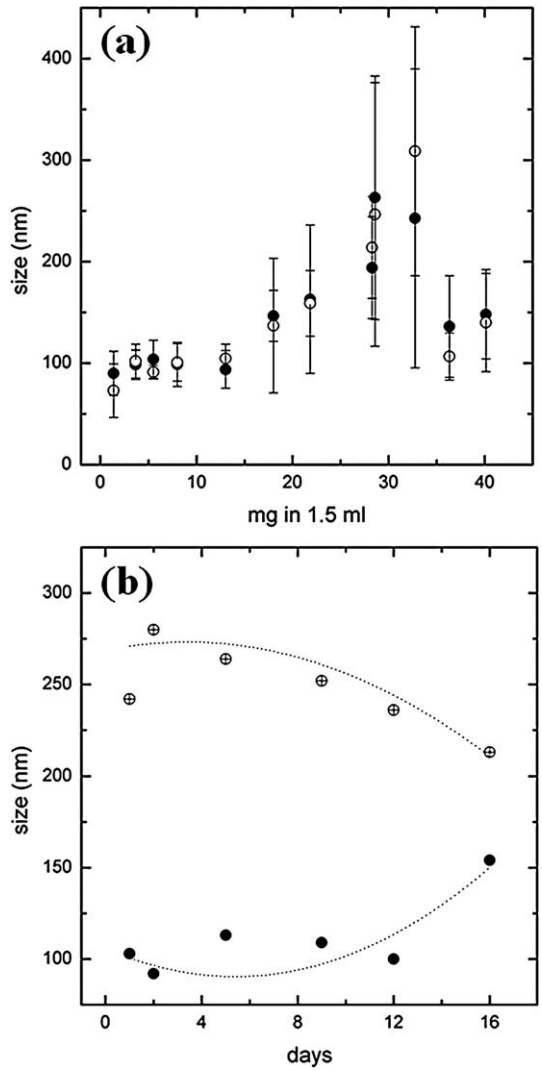

Fig. 2 (a) Size (diameter) of the ABA polymersomes at different polymer concentrations in aqueous solutions determined at room temperature. The filled and open circles represent the results measured two consecutive days. (b) Temporal evolution of the diameter for a sample above (open circles) and below (filled circles) 35 mg and 15 mg respectively.

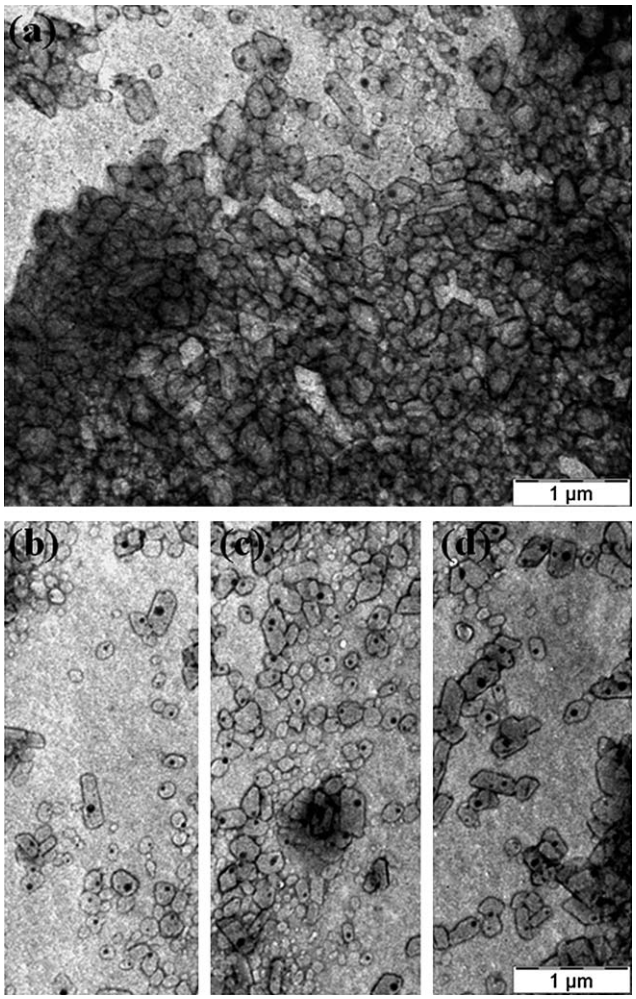

Fig. 3 TEM images of ABA block copolymer showing spherical and polyhedral vesicles in water solution: (a) A high density of collapsed polyhedral vesicles and (b,c) isolated polyhedral vesicles at a polymer concentration of 5 mg/mL. (d) Elongated polyhedral polymersomes at a concentration of 7.5 mg/mL.

with time from *ca.* 100 nm up to *ca.* 200 nm (see Fig. 2b). In contrast, for samples at concentration above this value the size decreases to mean sizes similar to those for the former samples. In both cases, we note an increase in polydispersity in such a way that samples are not homogeneous anymore after incubation.

In order to get additional information about the properties of the self-assembled copolymer structures in solution we performed TEM experiments. In Fig. 3 we show TEM images of a region with vesicles at different concentrations. These pictures confirm the structure variation with polymer concentration according to DLS data.

For concentrations lower than 5 mg/mL, classical spherical and polyhedral polymer vesicles or polymersomes of sizes *ca.* 90–150 nm are present, as shown in Fig. 3a–c. In particular, Fig. 3a shows some collapsed vesicles in some areas of the picture. The presence of polyhedral vesicles characterized by facetted faces is an indication of the crystallization of the ABA membranes after drying, as observed in Fig. 3b,c. The presence of a small dark spot in the body of the polyhedral polymersomes might indicate the collapse of an aristae of the polymersome membrane after drying or an excess of staining agent confined in the aqueous pool of the polymer vesicle before drying. It is necessary to note that not all the polymersomes display this dark spot. Differences in polymersome size if compared to DLS data might arise from partial dehydration (mainly the polymer corona) of the vesicles upon drying. As the copolymer concentration increases (7.5 mg/mL), a progressive elongation and fusion of the block copolymers vesicles can be observed (see Fig. 3d). The elongated structures seem to be formed by the fusion of polymeric vesicles and can be considered as a structural intermediate step from vesicles to tubular structures or nanotubes. This incomplete transition offers a strong support to the fusing process hypothesis to obtain tubular nanostructures, as also observed for other block copolymers and lipidic systems.[17]

In order to get further confirmation about the shape of intermediate structures associated to the spherical vesicle to tubular transition

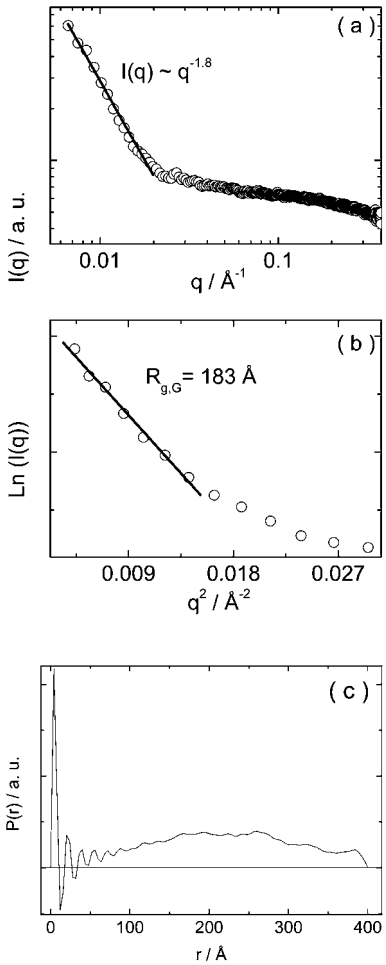

Fig. 4 (a) SAXS data collected showing a q-1.8 dependence of the intensity at low q. (b) Guinier plot for the SAXS data plotted in (a). The value calculated for $Rg_{,G}$ is indicated in the figure. (c) Distance distribution function calculated using the SAXS data plotted in (a).

SAXS experiments were performed. Fig. 4a shows the SAXS data measured for a sample containing 5 mg/mL copolymer. According to data in Fig. 4a, the intensity I(q) shows a $q^{-1.8}$ decay at low q, indicating the presence of layered structures, *e.g.*, vesicle walls.[18]

The SAXS data in Fig. 4a was used to calculate the Guinier plot for 5 mg/mL copolymer displayed in Fig. 4b. The Guinier plot in Fig. 4b presents only one Guinier region, showing that there is only one distribution of particle sizes in the system. A radius of gyration $R_{g,G} = 183$ Å, was calculated from the fitting of eqn (3) to the data in Fig. 4b. It is possible that $R_{g,G}$ is highly polydisperse, in keeping with the results displayed in the TEM (Fig. 3).

The distance distribution function of the system $p(r)$ for 5 mg/mL copolymer was calculated with the program GNOM,[19] using the SAXS data in Fig. 4a. The resulting $p(r)$, displayed in Fig. 4c, corresponds to a particle with a radius of gyration $R_{g,I} = 158$ Å. The good agreement within $R_{g,I}$ and $R_{g,G}$ (Fig. 4b) supports the consistency of the $p(r)$ calculation. The distance distribution function in Fig. 4c is characteristic of a hollow particle with strong positive-to-negative fluctuations within the shell. The thickness of the shell can be estimated from the value of r at which the $p(r)$ function passes from the large initial positive-

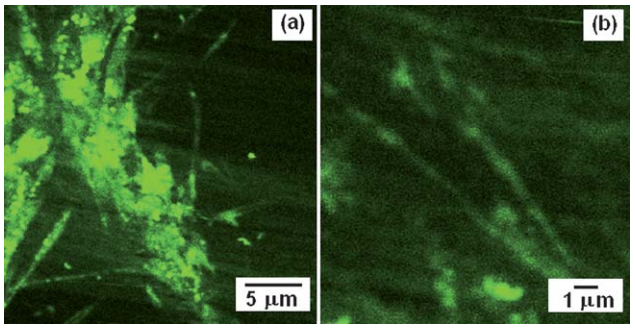

Fig. 5 LSCM for sample studied in Fig. 4.

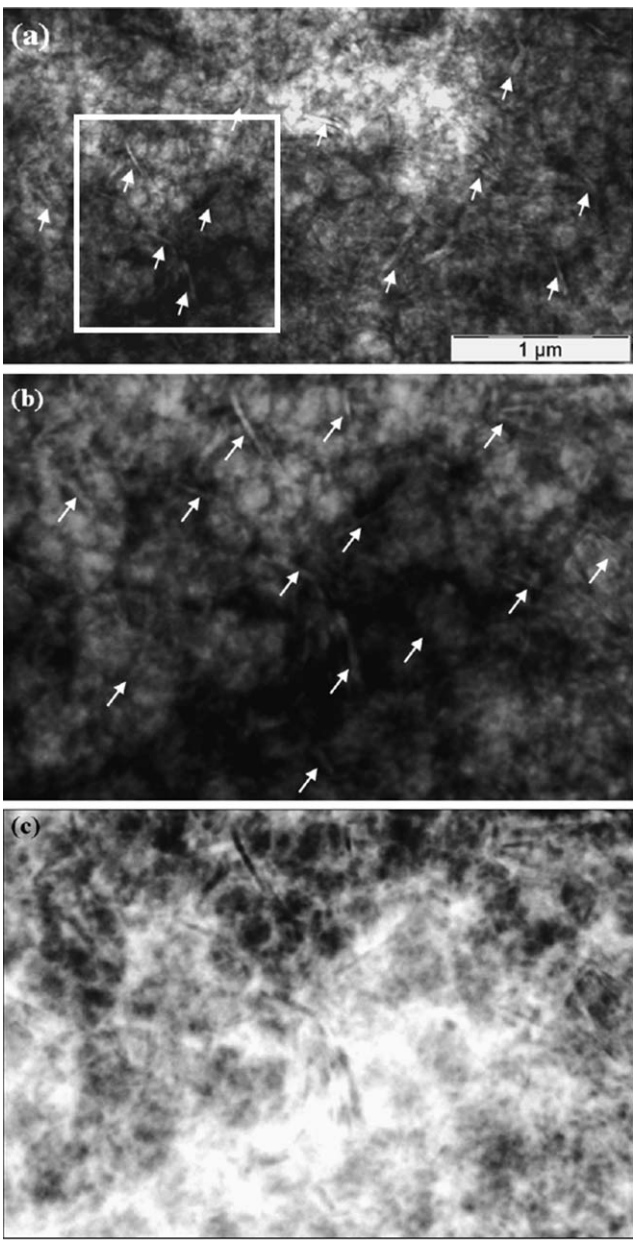

Fig. 6 (a) TEM image of a high density of tubular vesicles from and aqueous solution of ABA block copolymer at a concentration of 10 mg/mL. (b) High magnification image of a region from (a) (red square). (c) Inverted color image of (b). The white arrows highlight single tubular vesicles.

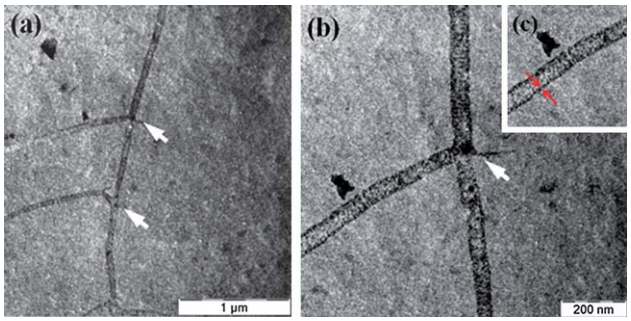

Fig. 7 (a) TEM image of a single tubular vesicle. The white arrow shows different y-junctions along the tubule. (b) Detail of a y-junction. (c) Estimation of the membrane thickness in a tubular vesicle.

negative oscillation into the adjacent ascending region of smaller oscillations.[20] According to Fig. 4c, the thickness of the shell is ~ 34 Å, such that the overall particle diameter (*i.e.* maximum distance measurable within the scattering particle) corresponds to Dmax = 400 Å. Dmax = 400 Å is considerably smaller that the polymersome sizes (900–1500) Å measured by DLS above for concentrations lower than 5 mg/ml. Indeed, the lower q value of the SAXS curve in Fig. 4a determines the maximum size of the particle which can be described through that SAXS curve. Then, although the SAXS data in Fig. 4a is useful to determine the thickness of the shell, it does not contain information about particle sizes bigger than $\sim(2\pi/q_o) = (2\pi/0.0066\ \text{Å}^{-1}) = 950$ Å. Thus, we hypothesize R_g measured by SAXS might correspond to the half width of the tubular aggregates formed in solution (that is, the small axis radius). Fig. 5 shows the LSCM results obtained for the sample studied by SAXS. The results denote the existence of elongated structures. Although it is difficult to determine the full length of these structures, the thickness can be estimated from Fig. 5, as corresponding to (406 ± 42) Å, in agreement with the R_g values measured by SAXS.

On the other hand, we also note that the length of the elongated structures increases as the polymer concentration rises to finally give tubular structures, which clearly appear when polymer concentration is around 10 mg/mL. Fig. 6 shows another region with a high density of tubular vesicles obtained from the same sample.

A large area of collapsed tubular vesicles is shown in Fig. 6a (see also Fig. 6b,c for magnification). The white arrows indicate single tubular vesicles over the whole area. The mean dimensions of the tubular polymersomes can be determined from these images, ranging between 400–700 nm in length and 30 nm in width, in fair agreement with the size increase observed from DLS data (which involves the assumption of considering a spherical particles in the theoretical analysis). Other ABA block copolymers have been used recently to form polymersomes with tubular conformation as the result of the conjunction of vesicles by reducing the medium temperature.[21] However, in our case both tubular and spherical polymersomes coexist at the same temperature.

In order to estimate the diameter and thickness of the tubular polymersomes and get more insight about the nature and structure of the assemblies formed by PMOXA-PDMA-PMOXA copolymer in aqueous solution we image a single tubular vesicle.

Fig. 7a shows a long tubular vesicle. The white arrows indicate the presence of y-junctions in the tubular structure. Fig. 7b shows a detail of a y-junction, and the white arrow points to a defect of a single ABA membrane going out of the body of the y-junction. A magnification of this picture allows estimation of the thickness of the tubular vesicle membrane around *ca.* 2 nm (see red arrows in Fig. 7c). This thickness was obtained by measuring the intensity profile between the red arrows as previously reported.[6a] Recently, Ma and Eisenberg[22] discussed the relation between size of the polymersomes and the thickness of the polymer membrane. According to these authors, for PS-*b*-PAA diblock copolymers the wall thickness decreases with decreasing vesicle size.

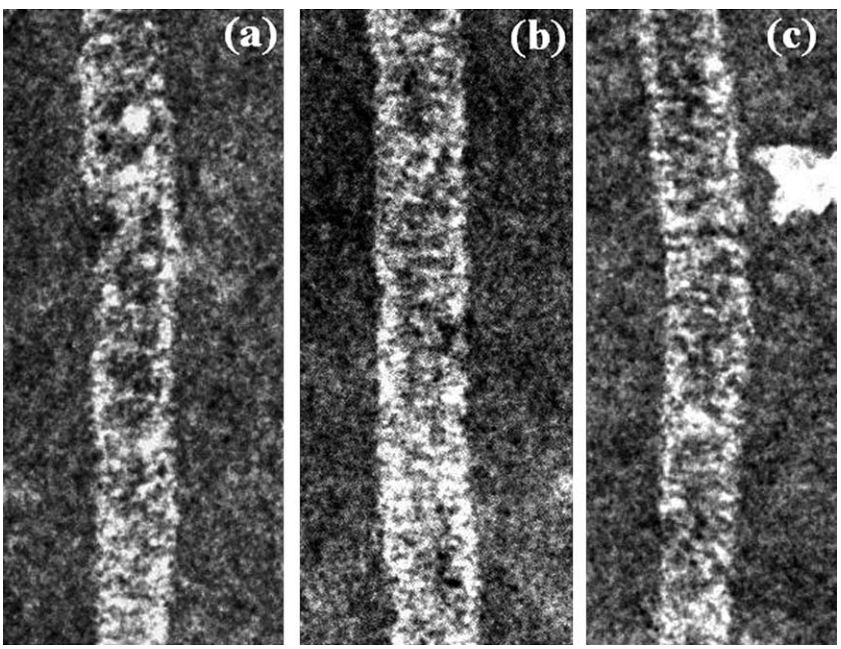

Fig. 8 (a–c) Details of single tubular vesicles in inverted colour-modes. The width of each image is 200 nm.

In order to get further insight about the properties of the ABA block copolymer vesicle membrane the nature of the polymer membrane was investigated by the analysis of different fragment of the tubular polymersomes.

Fig. 8a–c show both conventional and inverted colour-TEM pictures. The white arrows in Fig. 8a indicate fluctuations in the ABA block copolymer membrane, which seems to display discontinuities in its thickness. The membrane of the tubular vesicles also showed arrays of dark regions that could indicate different membrane thickness (Fig. 8b).

ABA deposition in solid supports

We intend to investigate the deposition and membrane formation of the PMOXA-PDMS-PMOXA copolymer on two solid supports: glass and mica. Both supports are negatively charged while our copolymer is electrically neutral. In order to form a suitable homogeneous membrane in a solid support we performed AFM experiments on the two supports by deposition of a stock copolymer solution of concentration 12.5 mg/mL. A drop deposited in the support was left to dry for two minutes and the excess of water removed by capillarity using filter paper. Finally the samples were imaged using AFM.

The first support under investigation was glass. This support shows a low surface charge density[23] that becomes lower after the solution is deposited onto the support. The remaining ions in solution attach to the solid support, thus decreasing the effective charge density. The results for the AFM imaging of the ABA polymer deposition in glass are shown in Fig. 9.

Fig. 9a shows a high density of fused elongated and spherical polymersomes which are not regularly packed, that is, clusters of vesicles are formed. Thus, the membrane formed displays a noticeable amount of defects as a consequence. In order to measure the mean size of the vesicle, we could image some isolated vesicles with the AFM instruments. Fig. 9b and c indicate the size of a selected vesicle as an example, with diameter of *ca.* 100 nm. Additional measurements on more vesicles indicate that their mean size from 100 to 200 nm with a noticeable

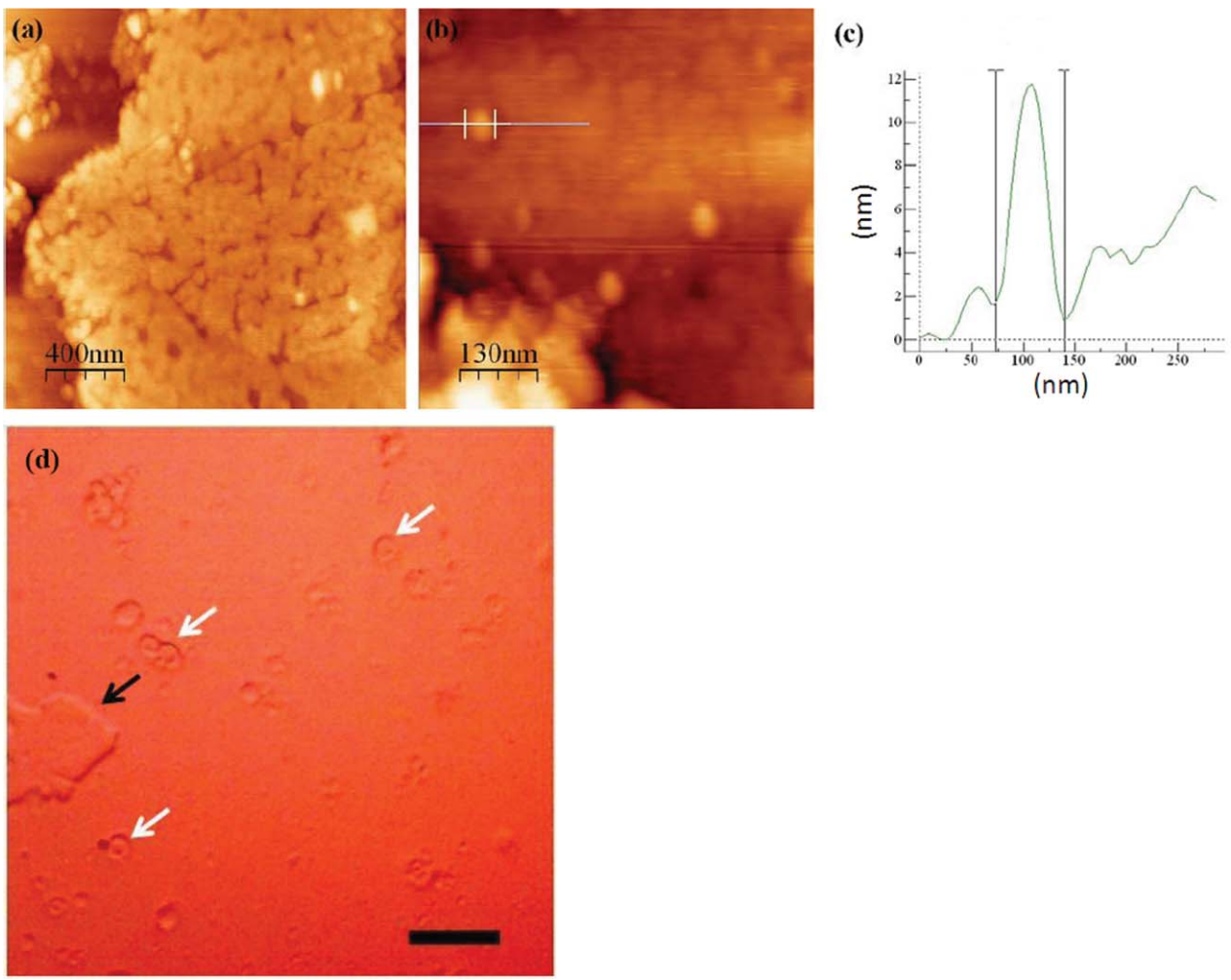

Fig. 9 (a) AFM picture denoting the matrix of ABA block copolymer polymersomes not uniformly distributed upon deposition onto a glass substrate. (b) AFM image of a single vesicle and (c) Height profile of the vesicle marked in (b) as an example deposited onto glass prepared at room temperature. The polymer concentration was 12.5 mg/mL. In (d) Optical microscopy image showing giant collapsed spherical polymersomes (white arrows) as well as large polymer films (black arrows) scale bar 25 μm.

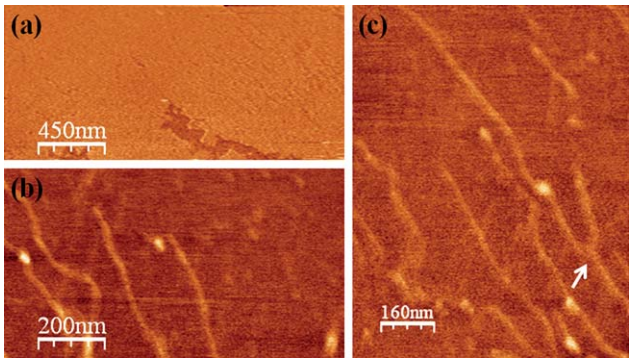

Fig. 10 Height AFM images of ABA block copolymer after deposition onto a glass support and a further washing step at room temperature: (a) Uniform copolymer layer with a defect in the bottom showing the solid support. (b,c) AFM pictures of tubular polymersomes. The white arrow in (c) denotes a y-junction. The copolymer concentration was 12.5 mg/mL.

polydispersity, in agreement with the size found in aqueous solution. Additionally experiments using an optical microscope have been performed. Using the same glass support and after a drying process we can show the presence of giant spherical deflated polymersomes as well as large polymer layers as is shown in Fig. 9d. In order to know if the irregular structure of the polymer film onto the glass support was a result of excessive polymer deposition, we also performed analogous experiments but including a final washing step of the polymer-loaded support before drying. After extensive washing, at least a great part of the aggregated material can be removed and, then, either individual tubular and spherical polymersomes can be observed, as well as obtaining a more uniform polymer layer. (See Fig. 10.)

In this case, Fig. 10a shows an apparently uniform polymer layer onto the support with few small defects. The membrane thickness was found to be about 2 nm (see Figure X2 in Supporting Information). Images of isolated polymersomes are also shown in Fig. 10b and c. Tubular polymersomes can be perfectly distinguished in these pictures besides some single spherical polymersomes, in agreement with TEM data. In Fig. 9c the white arrow shows the presence of a y-junction in good agreement with TEM images. The diameter of the tubular polymersomes was found to be about 40 nm.

For comparison, we also performed experiments on mica supports. Following the same protocol as the former experiments a drop of copolymer solution was deposited onto the support, left dried without the washing step and the results imaged using AFM.

Fig. 11a and b show the formation of an uniform membrane with several defects onto the mica support. The membrane on the mica support is homogeneous, and the analysis of the roughness on the top of the membrane and on clean mica gives values of 0.11 and 0.57 nm, respectively (see Figure X3 in Supporting Information). This is an indication of the good quality of the polymer membrane formed. After drying the membrane remains stable in the solid-air interface. The intensity profile in a region with mica and membrane is shown in Fig. 12. The thickness has a value of about 1.6 nm. Similar results in mica have been obtained by Rakhmatullina and Meier[24] using an ionic triblock block copolymer.

The membrane characteristics on the mica support without washing step are in contrast to those observed on a glass substrate, in which vesicle aggregation was observed. This different behaviour can be ascribed, on one hand, to the different effective negative electric charge carried by both kinds of supports.[23,25] which clearly influences the quality of the membrane formed. In particular, on mica the total number of negative lattice sites corresponds to one negative charge per 48 $Å^2$ or 2.1×10^{14} charges per cm^2, so the surface charge density is -0.33 C/m^2. In aqueous solution the value decreases several orders of magnitude because of the adsorption of cations on mica. This situation evidently affects the mechanism of membrane formation on the solid support because of the aqueous stock solution used for the membrane preparation. Also, the membrane formation is affected by the different strength and nature of the interactions between the copolymer molecules and the solid surfaces.[23,26]

We can conclude that using mica to support the deposited membrane leads to excellent properties of uniformity and low roughness suitable for membrane protein reconstitution in an

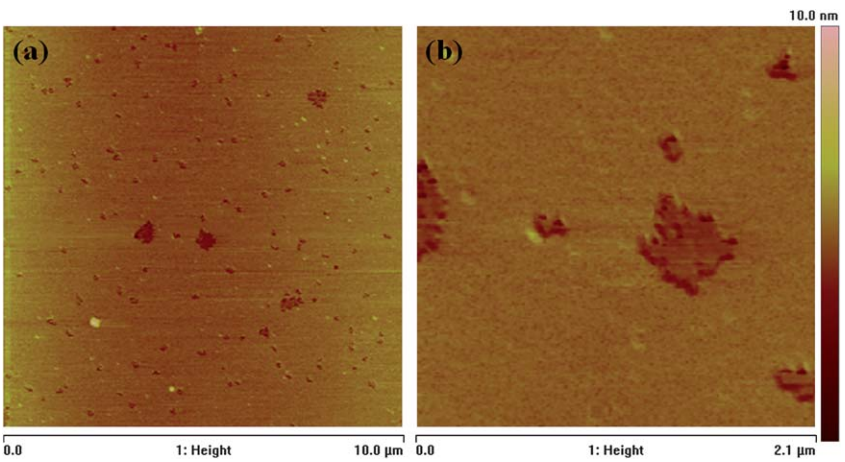

Fig. 11 Height AFM images of ABA block copolymer after deposition onto a mica support at room temperature in the absence of a washing step. (a,b) Uniform copolymer layer with the presence of some defects in its structure. The copolymer concentration was 12.5 mg/mL.

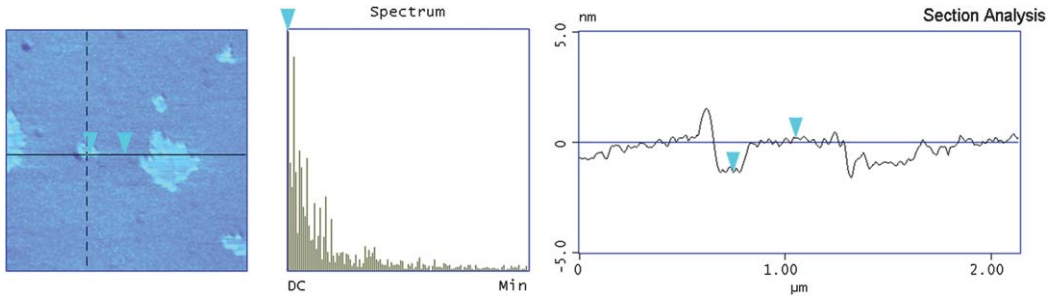

Fig. 12 (From left to right) Selected region, spectrum and height profile of the copolymer layer observed in Fig. 10.

analogous way to the free-standing ABA block copolymer membranes reported in our previous work.[10]

Conclusions

In the present work we characterize the self-assembled structures of an ABA block copolymer in aqueous solution and also the properties of the polymer films formed from these solutions upon deposition onto two different solid supports. The presence of spherical, polyhedral and tubular polymersomes was observed and found to be dependent upon polymer concentration in solution. Also upon drying, the formation of a uniform polymer membrane was found optimal for a mica support. These results open new possibilities to the incorporation of membrane proteins in solid-supported ABA polymer membranes from aqueous polymer solution, avoiding the disadvantages of using organic compounds, which can disrupt protein structure. The choice of the suitable solid support and ABA configuration is hence an important step to a successful membrane preparation. Further studies in membrane protein incorporation using mica as a support will be performed as a natural next step to investigate this system.

Acknowledgements

A. G.-P. wants to acknowledge Prof. Thomas Heimburg for giving him the opportunity to work in his group, and the Danish National Advanced Technology Foundation that funds Industrial Biomimetic Watermembrane Project (023-2007-1) for financial support between 1/05/2009 and 29/02/2010. A G-P would also like to acknowledge M. Alatorre-Meda, and M. M. Hermanowska and A, Gorska for their help in using the Nanoscope AFM and the Aligent PicoSPM AFM instrument in the Center for Biomembrane Physics (MEMPHYS) at the University of Southern Denmark, respectively. Work at Reading was supported by the EPSRC Platform Grant, ref. EP/G026203/1.

References

1 E. Munch, M. E. Launey, D. H. Alsem, E. Saiz, A. P. Tomsia and R. O. Ritchie, Tough, bio-inspired hybrid materials, *Science*, 2008, **322**, 1516–1520.
2 F. Xia and L. Jiang, Bio-inspired, smart, multiscale interfacial materials, *Adv. Mater.*, 2008, **20**, 2842–2858.
3 H. Lee, B. P. Lee and P. B. Messersmith, A reversible wet/dry adhesive inspired by mussels and geckos, *Nature*, 2007, **448**, 338–341.
4 I. W. Hamley. *The Physics of Block Copolymers*; Oxford University Press: New York, 1998.
5 I. W. Hamley. *Block Copolymers in Solution: Fundamentals and Applications*, Wiley, Hoboken, NJ, 2005.
6 (*a*) C. LoPresti, H. Lomas, M. Massignani, T. Smart and G. Battaglia, Polymersomes: nature inspired nanometer sized compartments, *J. Mater. Chem.*, 2009, **19**, 3576–3590; (*b*) X. Hou and L. Jiang, Learning from Nature: Building bio-inspired smart nanochannels, *ACS Nano*, 2009, **3**, 3339–3342.
7 R. Phillips, T. Ursell, P. Wiggins and P. Sens, Emerging roles for lipids in shaping membrane-protein function, *Nature*, 2009, **459**, 379–385.
8 (*a*) W. Meier, C. Nardin and M. Winterhalter, Reconstitution of channel proteins in (polymerized) ABA triblock copolymer membranes, *Angew. Chem., Int. Ed.*, 2000, **39**, 4599–4602; (*b*) M. Kumar, M. Grzelakowski, J. Zilles, M. Clark and W. Meier, Highly permeable polymeric membranes based on the incorporation of the functional water channel protein Aquaporin Z, *Proc. Natl. Acad. Sci. U. S. A.*, 2007, **104**, 20719–20724.
9 J. Grumelard, A. Taubert and W. Meier, Soft nanotubes from amphiphilic ABA triblock macromonomers, *Chem. Commun.*, 2004, 1462–1463.
10 A. Gonzalez-Perez, K. B. Stibius, T. Vissing, C. H. Nielsen and O. G. Mouritsen, Biomimetic triblock copolymer membrane arrays: A stable template for functional membrane proteins, *Langmuir*, 2009, **25**, 10447–10450.
11 (*a*) S. W. Provencher and P. Stepanek, Global analysis of dynamic light scattering autocorrelation functions, *Part. Part. Syst. Charact.*, 1996, **13**(5), 291–294; (*b*) P. Stepanek and S. W. Provencher, Global analysis of correlation functions: Dynamic light scattering from polymers and block copolymers, *Macromol. Symp.*, 2000, **162**, 191–203.
12 I. Horcas, R. Fernandez, J. M. Gomez-Rodriguez, J. Colchero, J. Gomez-Herrero and A. M. Baro, WSXM: A software for scanning probe microscopy and a tool for nanotechnology, *Rev. Sci. Inst.*, 2007, **78**, 013705-1–013705-8.
13 A. Guinier., *X-ray Diffraction*, W. H. Freeman, San Francisco, 1963.
14 A. Guinier; G. Fournet., *Small-Angle Scattering of X-rays*, John Willey & Sons Inc., New York, 1955.
15 O. Glatter; O. Kratky., *Small Angle X-ray Scattering*, Academic, London, 1982.
16 K. Kita-Tokarczyk, J. Grumelard, T. Haefele and W. Meier, Block copolymer vesicles - using concepts from polymer chemistry to mimic biomembranes, *Polymer*, 2005, **46**, 3540–3563.
17 (*a*) J. W. Y. Lam and B. Z. Tang, Functional polyacetylenes, *Acc. Chem. Res.*, 2005, **38**, 745–754; (*b*) Z. Tian, H. Li, M. Wang, A. Zhang and Z.-G. Feng, *J. Polym. Sci., Part A: Polym. Chem.*, 2008, **46**, 1042–1048; (*c*) P. Xu, G. Tan, J. Zhou, J. He, L. B. Lawson, G. L. McPherson and V. T. John, *Langmuir*, 2009, **25**, 10422–10425.
18 O. Glatter. The Inverse Scattering Problem in Small-Angle Scattering. *In Neutrons, X-rays, and Light: Scattering methods applied to soft condensed matter*, ed. P. Lindner, and T. Zemb, Elsevier, Amsterdam, The Netherlands, 2000.
19 D. I. Svergun, *J. Appl. Crystallogr.*, 1992, **25**, 495–503.
20 P. Laggner, A. M. Gotto and J. D. Morrisett, *Biochemistry*, 1979, **18**, 164–171; P. Laggner, O. Glatter, K. Muller, O. Kratky, G. Kostner and Q. A. Holasek, *Eur. J. Biochem.*, 1977, **77**, 165–171.
21 Z. Tian, H. Li, M. Wang, A. Y. Zhang and Z. G. Feng, Vesicular and tubular structures prepared from self-assembly of novel amphiphilic ABA triblock copolymers in aqueous solutions, *J. Polym. Sci., Part A: Polym. Chem.*, 2008, **46**, 1042–1050.
22 L. Ma and A. Eisenberg, Relationship between wall thickness and size in block copolymer vesicles, *Langmuir*, 2009, **25**, 13730–13736.

23 E. Rakhmatullina and W. Meier, Solid-supported block copolymer membranes through interfacial adsorption of charged block copolymer vesicles, *Langmuir*, 2008, **24**, 6254–6261.
24 S. H. Behrens and D. G. Grier, The charge of glass and silica surfaces, *J. Chem. Phys.*, 2001, **115**, 6716–6721.
25 G. L. Gaines and D. Tabor, Surface adhesion and elastic properties of mica, *Nature*, 1956, **178**, 1304–1305.
26 (*a*) A. Galliano, S. Bistac and S. Schultz, Adhesion and friction of PDMS networks: Molecular weight efects, *J. Colloid Interface Sci.*, 2003, **265**, 372–379; (*b*) T. Haefele, K. Kita-Tokarczyk and W. Meier, Phase behavior of mixed Langmuir monolayers from amphiphilic block copolymers and an antimicrobial peptide, *Langmuir*, 2006, **22**, 1164–1172.

